



The role of nano-scale heterogeneous electrostatic interactions in initial bacterial adhesion from flow: A case study with *Staphylococcus aureus*

Surachate Kalasin^a, Jeffrey Dabkowski^c, Klaus Nüsslein^b, Maria M. Santore^{c,*}

^a Department of Physics, University of Massachusetts, Amherst, MA 01003, United States

^b Department of Microbiology, University of Massachusetts, Amherst, MA 01003, United States

^c Department of Polymer Science and Engineering, University of Massachusetts, 120 Governors Drive, Amherst, MA 01003, United States

ARTICLE INFO

Article history:

Received 20 September 2009

Received in revised form

13 December 2009

Accepted 15 December 2009

Available online 22 December 2009

Keywords:

Bacterial adhesion

Protein film

Biofouling

Gravity-free

ABSTRACT

This study investigated the initial adhesion of *Staphylococcus aureus* from flowing buffer onto modified albumin films with the objective of probing the influence of electrostatic heterogeneity on bacterial adhesion. Electrostatic heterogeneity, on the lengthscale of 10–100 nm, was incorporated into the protein film through the irreversible random deposition of small amounts of polycation coils to produce isolated positive “patches” on the otherwise negative albumin surface before exposure to bacteria, which also possess a net negative surface charge. The system was benchmarked against an appropriate analog using 1 μm silica spheres and the same cationic patches on a silica substrate. Bacterial adhesion from flow was measured with the surface oriented vertically to eliminate gravitational forces between the bacteria and collector. In both systems, a threshold in the surface density of polycation patches needed for bacterial (or silica particle) capture indicated multivalent binding: multiple polycation patches were needed to adhere the bacteria (particles). The shifting of the threshold to greater patch concentrations at lower ionic strengths confirmed that the electrostatic interaction area (zone of influence) was a key factor in modulating the interactions. The role of the contact area in this manner is important because it enables a quantitative explanation of counterintuitive bacterial adhesion onto net negative surfaces. The study further revealed a hydrodynamic crossover from a regime where flow aids bacterial adhesion to one where flow impedes adhesion. An explanation is put forth in terms of the relative hydrodynamic and surface forces.

© 2009 Elsevier B.V. All rights reserved.

1. Introduction

Interest in bacterial adhesion has transcended the biomedical community due to the importance of the topic to medical implants, membrane fouling, and bacterial transport in groundwater. Engineering studies employing indirect methods revealed several unequivocal conclusions: non-specific interactions usually produced adhesion into the secondary minimum of the bacterial-surface potential [1,2]. Also, surface heterogeneities increased bacterial adhesion over predictions by DLVO (Derjaguin, Landau, Verwey, and Overbeek) or extended DLVO theories [1,3–7]. Additionally, variations in the growth phase and composition of the bacteria’s lipopolysaccharide layer created variations in the adhesion of otherwise similar strains [3,4,7]. Further, an ionic strength-dependent critical flux separated conditions for reversible and irreversible bacterial deposition from flow, evidencing intricate hydrodynamic effects [8,9].

Direct measurements of bacterial adhesion via AFM or controlled flow/particle tracking have corroborated the engineering studies. Electrostatic, dispersion, donor–acceptor, hydrodynamic, and biomolecular interactions were quantified for bacterial capture and removal through a number of routes including shearing flow, impinging jet, and bubble flow methods, with data for several bacterial strains and substrate chemistries summarized [10]. There was a general lack of correlation between forces of bacterial capture and removal from a surface, reinforcing fundamental differences between the two processes, with order pico-Newton forces involved in the former and order 10–100 pN forces involved in the latter [10–14]. Non-specific interactions, sufficient to capture and hold bacteria on many surfaces [13,15,16], generally preceded biomolecular recognition, which further increased adhesion by about a factor of 2–4 [10,17–22]. The more direct studies reinforced the disparity between DLVO or extended DLVO calculations and experiments, with greater bacterial adhesion due to roughness [18] or charge heterogeneity [6,19,23].

The current paper quantifies how nanoscale heterogeneities in electrostatic charge, which are systematically varied, produce sharp attractions between bacteria and surfaces of the same net

* Corresponding author.

E-mail address: santore@mail.pse.umass.edu (M.M. Santore).

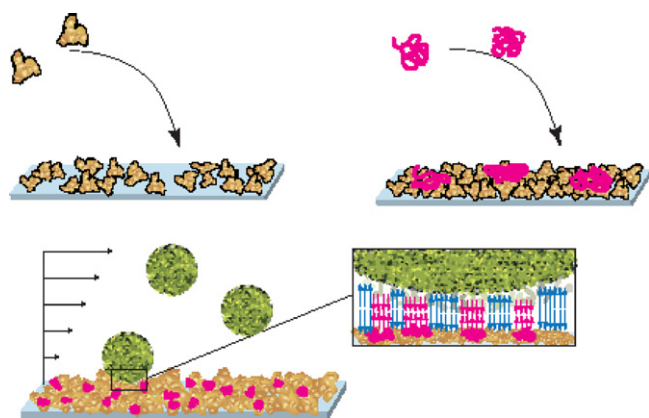


Fig. 1. Top: deposition of polycation patches on an albumin film. Below: flowing bacteria over cationically patchy BSA-surfaces: each bacterium experience competing electrostatic attractions and repulsions that determine whether it ultimately adheres.

charge. In practice, charge heterogeneity is likely to exist on the bacteria surface *and* on protein-coated substrates. This paper focuses on the latter because, while charge heterogeneities on bacterial surfaces are well-accepted [1,3,4], they are not characterized in terms of their lengthscales and distributions to the extent necessary for quantitative prediction of bacterial adhesion.

The current work demonstrates the importance of competing attractive and repulsive interactions, separated spatially on a surface, in controlling bacterial adhesion during initial encounter. Evidence is presented that adhesion is governed by an effective electrostatic contact region between a bacterium and the surface, tunable through ionic strength. Also demonstrated is an adhesion threshold which parallels that seen for silica particle deposition, suggesting that other features of silica particle adhesion likely apply to bacterial adhesion as well. Finally, the influence of flow on heterogeneity-facilitated bacterial capture is investigated.

2. Experimental strategy

This study develops an albumin-based surface as a model substrate for bacterial adhesion, in Fig. 1. Negatively charged albumin films are modified by small but tightly-controlled amounts of randomly and irreversibly-adsorbed 10 nm polycation (polydimethyl aminoethyl methacrylate, pDMAEMA) chains. At sparse surface loadings, isolated polycation coils create adhesive cationic “patches” on the non-bioadhesive negative albumin surface. The adhesion of *Staphylococcus aureus* from flow onto these surfaces is then studied.

The interpretation of bacteria–surface interactions is facilitated by comparison to a well-characterized control comprised of silica flats with similarly-deposited polycation (pDMAEMA) coils [24,25]. Previous characterization of this composite surface revealed the strong locally cationic character of the adsorbed patches [26], which were about 10 nm in size [25], and flat to the surface [27,28], with confirmed random surface arrangement [29]. Polycation patches were retained on silica flats in flowing buffer, and on exposure to proteins and silica particles [24,30–32].

The electrostatic repulsion between 1-micron silica spheres and the polycation-modified silica flats runs parallel to the bacteria–albumin film interactions: in the absence of adsorbed polycation coils neither the silica spheres nor the *S. aureus* adhere to their respective substrates. Indeed this was the basis for choosing albumin layers as the main substrate for bacterial adhesion, since we find flowing *S. aureus* did adhere to silica flats. A second parallel between the two systems is the spherical nature of *S. aureus* and its negative charge, though *S. aureus* surfaces are known to be heterogeneous.

The silica control system has formed the basis for a quantitative understanding of microparticle capture on heterogeneously-charged surfaces, with explanations of (1) a compositional threshold for substrate features producing particle adhesion [24,25], (2) the influence of ionic strength on particle capture including a retrograde region of salt-reduced adhesion [29] and (3) a crossover in the effect of flow on particle capture from the case where flow hindered particle capture to that where capture was aided by flow [33]. While the albumin-coated substrates are relevant to biomedical devices which are quickly coated with proteins, the silica system is relevant to diagnostic chips. Notably, the films on biomedical implants contain protein mixtures where a fraction of them are responsible for bacterial adhesion. By employing cationic polymer patches, the current study focuses on well-controlled electrostatically attractive regions that also might be found in an adsorbed protein layer. (While many proteins are net-negative, some of them contain positively charged domains. Due to dominance by its central positive domain in certain cases, fibrinogen behaves qualitatively similarly to the electrostatic patches of the current work with regards to silica particle capture [34].)

3. Experimental description

Bovine serum albumin (cat #A7511, fatty acid free) was purchased from Sigma and used as-is. pDMAEMA (31,300 molecular weight, PDI = 1.2) was a gift from DuPont and transferred from its original methanol solution as needed by rotovaporation to water. Each batch was characterized for completeness of solvent removal by ^1H NMR. Glass substrates were microscope slides (Fisher Finest) soaked in concentrated sulfuric acid overnight, and rinsed with substantial amounts of deionized (DI) water, a procedure shown to remove metal ions from the near surface region and leave a silica surface with a thickness near 10 nm [35]. 1 μm monodisperse silica spheres were purchased from GeTech (Orlando).

S. aureus bacteria (ATCC 25923) were grown in Luria-Bertani (LB) medium per standard procedures. The cultures were incubated aerobically overnight at 37 °C, with shaking at 200 rpm and harvested after a total of 24 h during logarithmic growth. To provide bacterial suspensions free of protein and other polymeric material which might adsorb to our surfaces, suspensions were centrifuged at 3000 rpm (1000 \times g) and cells resuspended in phosphate buffer, a procedure which was conducted twice. The final bacteria concentration for adhesion studies was 5×10^8 cells/ml. All bacteria were used within 24 h of preparation and stored in a refrigerator near 4 °C. The strain was originally a clinical isolate, and is today widely used in standardized tests of bacterial antibiotic susceptibility. This particular strain was chosen for its non-pathogenic behavior, while still closely resembling strains found in hospital infections.

Planar substrates were prepared by sealing a microscope slide in a slit shear flow chamber [36,37], equilibrating with flowing buffer, and then flowing the solutions of interest over the surface to permit adsorption. In studies of the deposition process, Near-Brewster Optical Reflectometry was employed to track protein and polymer adsorption. Our custom-built reflectometer employs an internal reflection configuration that brings the 633 nm parallel-polarized probe beam from a He Ne laser to the interface through the optically clear substrate slide [35]. Near the Brewster angle for a perfect interface, the reflected beam vanishes. Small amounts of adsorbing molecules are easily detected at these conditions, with the reflected beam intensity scaling as the square of the interfacial mass. The optical calibration constant for the various layers is determined from their refractive indices, as previously described [35].

Patchy surfaces were created by flowing a 20 ppm buffered pDMAEMA solution for varied amounts of time (0.1–5 min) dur-

ing which adsorption occurred, and then switching back to buffer, to limit the amount of patches on the surface. (The buffer for surface preparation and protein/polycation adsorption was 0.008 M Na_2HPO_4 plus 0.002 M KH_2PO_4 with these compounds from Fisher. Its ionic strength, I , was 0.026 M.) In the case of modified albumin films, a nearly saturated layer of albumin was first adsorbed, as shown below, and following 10 min of buffer flow, the pDMAEMA patches were deposited. The pDMAEMA was strongly attracted to both silica and the albumin films so that its deposition was transport limited (and therefore the rate was quantitatively reproducible). Careful timing of the pDMAEMA adsorption led to tight control ($\pm 0.02 \text{ mg/m}^2$) of the pDMAEMA coverage, as previously established. Also, we generally found that, at the pH and ionic strength of interest, the surfaces were stable during subsequent solvent flow and bacterial/particle adhesion studies.

Worth mentioning, the areal percentage coverage of the surface by the pDMAEMA patches coincidentally matches the % mass coverage relative to saturation. This is the case because of the dominance of trains in adsorbed pDMAEMA [27]. The surface density of cationic patches is described, therefore, as percentage coverage rather than loading in mg/m^2 , though the two are linearly proportional. Also, the average center–center patch spacing, derives from knowledge of the adsorbed amount (mg/m^2) and the polymer molecular weight.

Bacterial adhesion was recorded on DVD at standard video capture rates (30 frames/s) through the $20\times$ objective of a “lateral microscope”, a custom-built microscope oriented horizontally on our optical bench so that the surface of interest is oriented vertically. In this way, gravity did not contribute to the bacteria–surface forces. Other studies, to our knowledge, investigate bacterial adhesion on the floor [12,38] and/or the ceiling [10] of test chambers, and present combinations of the individual adhesion traces and the average [39]. The latter does not rigorously correspond to the situation of gravity-free transport and adhesion.

Like the studies of albumin and pDMAEMA adsorption in the slit shear flow chamber in the reflectometer, a glass flow chamber of similar dimensions was employed in the lateral microscope [36,37]. Bacterial adhesion was initiated by flowing buffer over the surface of interest for 10 min, and, following a valve turnover, bacteria were pumped through the flow chamber and their deposition monitored. Buffers for bacterial adhesion included the $I = 0.026 \text{ M}$ buffer from the polymer/protein deposition, or the same buffer diluted to $I = 0.005 \text{ M}$. Bacterial accumulation on the surface, as a function of time was quantified using Image J software.

Most bacterial adhesion traces were run twice some thrice, days apart with different preparation batches of bacteria, with random ordering of the cationic surface loading (i.e. in Fig. 5). Overall ten batches of bacteria were used in the bacterial capture studies. The random ordering of the runs with regard to cation density avoided possible artifacts arising from bacterial age, cell death.

Zeta potential studies to characterize the adhesive substrates were conducted using $1\text{-}\mu\text{m}$ silica particles to approximate the electrostatic character of the planar surfaces. The silica spheres were weighed carefully, so that the surface area within each sample was known precisely. Then, the appropriate amount of pDMAEMA, or albumin followed hours later by pDMAEMA, was added. The dispersions were allowed to equilibrate at least overnight so that all free molecules had a chance to adsorb to the surfaces before measurements were made. Given that both the BSA and the pDMAEMA were found, in reflectometry, to be strongly adsorbing on the silica, with the particles it was assumed that all free molecules eventually adsorbed to the surface of the silica spheres (whose area was designed to be at least an order of magnitude greater than the wetted area of the container). (We do not report measurements for suspensions in which more than the saturation amount of polycation or albumin was added.) Zeta potential measurements were

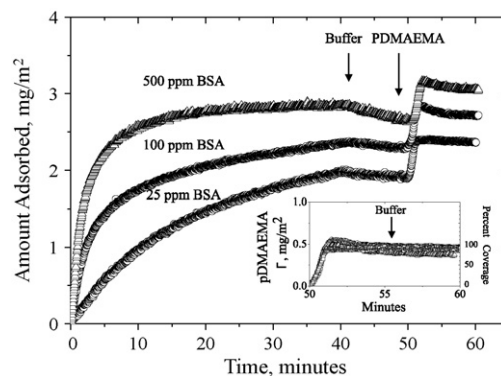


Fig. 2. Reflectometry traces for BSA adsorption on silica flats at 3 BSA concentrations, followed by pDMAEMA adsorption from a 20 ppm solution. During all portions of the run, the pH is 7.4 and the ionic strength is 0.026 M. The wall shear rate is 5 s^{-1} . The inset superposes the pDMAEMA portions of the 3 runs to illustrate that pDMAEMA adsorption is insensitive to the underlying albumin coverage. Also superposed in the inset is the adsorption of pDMAEMA on bare silica at the same pH and ionic strength, nearly indistinguishable.

conducted on a Malvern Zetasizer Nano ZS instrument, with at least 5 measurements averaged for each data point. Distributions were examined to ensure that each sample contained only a single sharp peak in particle mobility. Bacterial zeta potentials were measured as a function of ionic strength in a similar fashion.

4. Results and discussion

4.1. Creation and characterization of patchy surfaces

pDMAEMA adsorption over a saturated adsorbed albumin layer in Fig. 2 is similar to its adsorption on bare silica, suggesting similar structures in the two classes of polycation-containing surfaces. In Fig. 2, the albumin adsorption rate and coverage depend on free albumin concentration, previously shown to result from a competition between the rates of albumin arrival to the surface and albumin denaturing [40,41]. The latter increases the molecular footprint and excludes other albumin molecules. Since previous studies [40,41] suggest complete surface coating at these different albumin coverages, we find that the choice of albumin adsorption conditions is not critical. In the bacterial adhesion studies, we ultimately chose to adsorb albumin films from a concentration of 100 ppm.

Fig. 2 also demonstrates that (1) albumin adsorption is irreversible on the practical timescale of interest, (2) pDMAEMA adsorption on top of albumin proceeds in a quantitatively similar fashion, regardless of how the albumin was originally laid down and (3) in the inset, the coverage and kinetics of the pDMAEMA adsorption on top of albumin proceed similarly to that on bare silica. All these observations suggest similarities between the pDMAEMA on albumin and bare silica surfaces. The quantitative similarity of the pDMAEMA adsorption traces on silica and albumin suggest that albumin is not displaced by pDMAEMA. Further, of relevance for future studies with this system, we did not find significant loss of adsorbed mass when 0.15 M NaCl was added to the buffer.

The patchy electrostatic nature of the collecting surfaces is the key feature of interest in the current study. Zeta potential measurements in Fig. 3 demonstrate how the surfaces of $1 \mu\text{m}$ silica spheres or silica spheres with an albumin layer are incrementally altered by increased amounts of adsorbed pDMAEMA. At two ionic strengths, the underlying negative silica charge is ultimately overcompensated by a saturated pDMAEMA layer adsorbed directly on the silica. At intermediate pDMAEMA coverages, the surface must consist of regions of positive and negative charge, with the former comprising pDMAEMA and the latter made of exposed silica. The

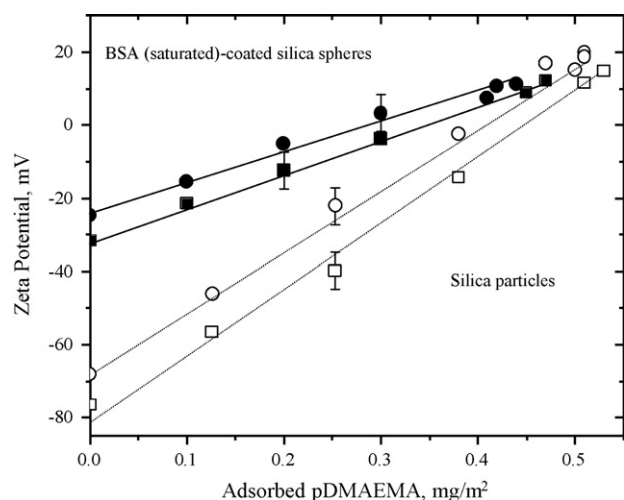


Fig. 3. Zeta potentials of pDMAEMA adsorbed onto 1- μm silica particles or 1- μm silica particles previously saturated with adsorbed albumin. The squares represent $I = 0.005$ M while circles represent $I = 0.026$ M. Characteristic error bars are shown. Lines have been drawn to guide the eye. The pH is pH 7.4.

linearity of the data demonstrate that each pDMAEMA patch added to the surface brings with it the same amount of positive charge, so that the electrostatic nature of each patch is not influenced by others on the surface.

Also in Fig. 3, the adsorption of pDMAEMA on an albumin film behaves similarly to pDMAEMA on bare silica. The primary difference is that the magnitude of the zeta potential of the pre-adsorbed albumin film (on the y-axis) is smaller than that of bare silica, though both the albumin and silica are negative. Again, the linearity of the zeta potentials of pDMAEMA on top of albumin again suggests that the per-patch level of cationic charge is fixed and independent of the patch concentration on the surface. Finally, the close similarities of the zeta potentials of the fully saturated pDMAEMA layer on bare silica versus on the albumin film suggest that on the latter, the polycation does not migrate substantially into or beneath the protein layer.

4.2. The adhesion threshold

Fig. 4 presents a series of bacterial adhesion runs on albumin films which contain varied amounts of cationic patches. In these experiments, buffer flowing gently over the various substrates at a wall shear rate of 22 s^{-1} was switched to a bacterial suspension

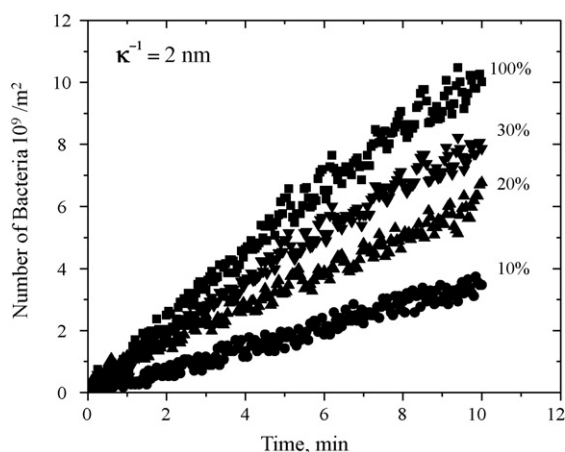


Fig. 4. Adsorbed amount of bacteria as function of time for different pDMAEMA loadings adsorbed on top of a saturated albumin layer, $I = 0.026$ M, pH 7.4.

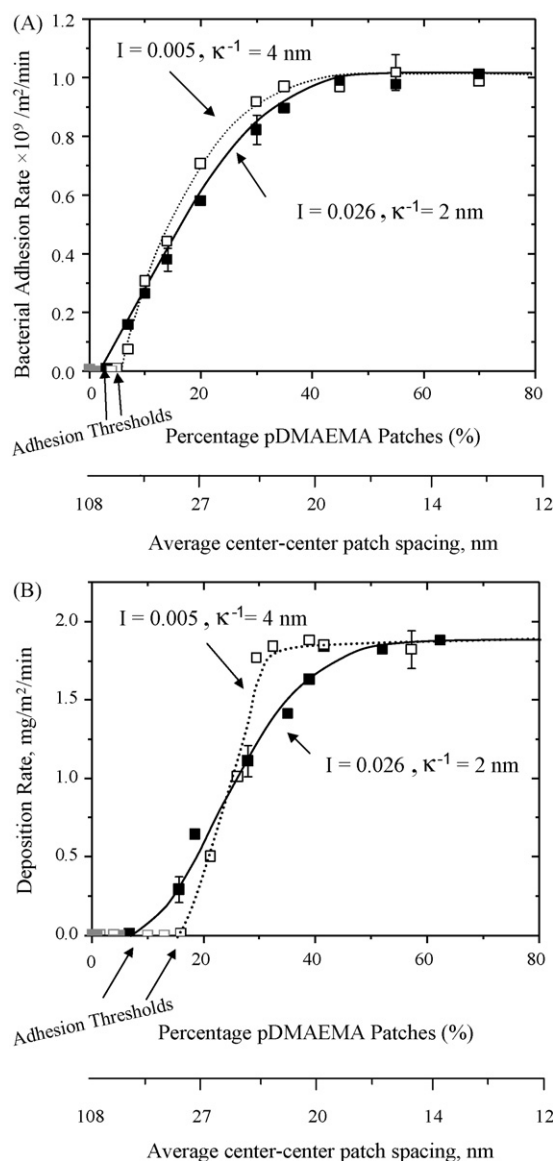


Fig. 5. (A) Deposition rates of *S. aureus* bacteria onto albumin layers containing different densities of pDMAEMA patches on the x-axis. Data for two ionic strengths are provided: 5 and 26 mM, pH 7.4. Curves are drawn to guide the eye, with characteristic error bars. Grey points on the x-axis below the adhesion thresholds indicate no bacterial adhesion. (B) Deposition rates of 1 μm silica particles on a silica flat carrying different adsorbed amounts of pDMAEMA, on x-axis. Data are shown for 2 ionic strengths. Data reproduced from Ref. [29].

of 5×10^8 cells/ml and deposition monitored in time. In Fig. 4, the adhesion of flowing bacteria increases linearly in time, for 10 min and beyond. For the most adhesive surfaces, the maximum coverage at this time, $10 \text{ cells} \times 10^9/\text{m}^2$, corresponds to an areal coverage of 0.8%. At these conditions, bacteria already adhering to the surface are too sparse to influence the capture of subsequent bacteria, rendering the deposition rate a good measure of net bacteria–substrate interactions.

Fig. 5A, the rate of bacterial deposition as a function of collector composition, summarizes the slopes of data such as that detailed in Fig. 4, along with additional runs for 2 different ionic strengths. Most data are the average of two runs, with typical error bars similar to the sizes of the points themselves. A few error bars are shown for example. Several features are worth noting: first, bacterial adhesion generally increases with the density of cationic patches on the x-axis. For the gentle flow of 22 s^{-1} , these bacteria are entirely non-adherent on albumin films, on the left side of

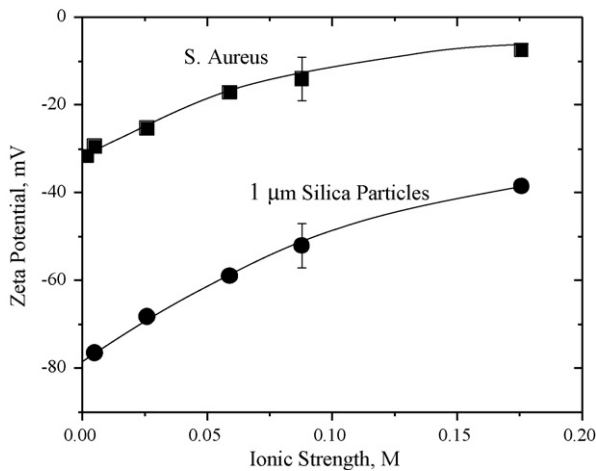


Fig. 6. Zeta potentials of *S. aureus* ATCC 25923 and 1 μm silica particles as a function of ionic strength, at pH 7.4. Characteristic error bars are shown.

the plot. On the right hand side, the bacterial adhesion rate levels off at that quantitatively corresponding to the transport limit, as predicted by Leveque [42]. At intermediate surface compositions, bacterial adhesion is influenced by the density of cationic patches on the surface. In Fig. 5B, similar adhesion signatures are seen for the adhesion of 1 μm silica spheres on a silica collector carrying varied concentrations of the same cationic patches.

Two general features of Fig. 5 are noteworthy: first, the transport-limited adhesion rate of bacteria or silica, seen for substantially cationic surfaces on the right sides of the graphs, persists for surface compositions with are electrostatically repulsive, in Fig. 5A below $\sim 0.3 \text{ mg/m}^2$, or $\sim 60\%$ patches on albumin or in Fig. 5B below 0.4 mg/m^2 or 80% patches on silica. Once a bacterium (or silica sphere) diffuses to the near-surface region, the time needed for its escape is generally longer than the time it takes to find an attractive surface region: though the surface is net negative, there are still many attractive regions due to the cationic patches.

The second important feature in Fig. 5 is adhesion threshold behavior for bacteria and microsphere accumulation. That is, bacteria and microspheres do not adhere at all on surfaces containing small amounts of patches. Rather, adhesion takes place only above a threshold in surface composition, in the range of a few percent patch coverage. This indicates that multiple patches are involved in the capture of each bacterium or microsphere. To see this, consider the possibility (which was observed *not* to occur), that the data intersect the origin rather than the x -axis. Then all surfaces containing polycations, however sparse, would be capable of capturing bacteria/particles. In this case, a single patch, on the electrostatically-repulsive albumin-coated surface, would be able to capture a particle, albeit very slowly. The fact that this was not observed, however, suggests that instead of particles captured by single patches, they are captured cooperatively by multiple patches. A similar argument has been established for the microparticles [25,29]. The slightly larger threshold values for the silica spheres are expected because the negative charge on the silica collector is stronger than that on the bare albumin film, in Fig. 3. Further, the negative charge on the flowing silica spheres is stronger than that on the bacteria, in Fig. 6. Greater densities of cationic patches are therefore needed to overcome silica sphere repulsion to the silica flat compared with bacterial repulsion from the albumin film, giving the larger threshold for the silica system.

4.3. Influence of salt and importance of contact area

Fig. 5A demonstrates that as the salt concentration is increased, the adhesion threshold becomes smaller and the impact of patch

density more gradual. The smaller adhesion threshold suggests a shifting of the system towards (but not yet reaching) the situation where the binding energy of individual patches (on the particular repulsive background of an albumin film) is sufficient to capture bacteria. Also seen with changes in ionic strength is a crossing of data sets.

These features are qualitatively identical to those seen with a silica sphere interacting with a silica-based patchy surface, in Fig. 5B. Critical in that model system, and apparently equally important for bacterial adhesion is the effective contact area between the particle (or bacterium) and the surface. This area, termed the “zone of influence” in our previous work [24,25,29], is illustrated in Fig. 7: when a sphere interacts electrostatically with a flat surface, the region of the flat that exerts force on the sphere is determined by the intersection of the flat with a shell of thickness κ^{-1} (the Debye length) around the sphere. The radius of the zone of influence is $R_{\text{zoi}} = 2(R_p\kappa^{-1})^{1/2}$, with R_p , the radius of the rigid sphere.

Small Debye lengths produce small zones of influence so that particles and bacteria are highly sensitive to the surface charge fluctuations. Thus, at high salt concentrations, bacteria and particles adhere to regions containing above-average densities of cationic patches, despite the net negative surface character. At low salt concentrations, particles and bacteria sample a more nearly average (net repulsive) surface character. Therefore, greater amounts of cationic patches are needed for the particles/bacteria to adhere, shifting the threshold to the right.

It was shown with silica spheres that the effect of salt on the interactive area is more important than its direct effect on the range of the interactive potential and resulting change in DLVO energy barrier height. Though the latter decreases with added salt to produce adhesion, the contact area effect reinforces and dominates the energy barrier effect [29]. In the current system, modest changes in Debye length (from 2 to 4 nm in Fig. 5) translate to large changes in the electrostatic contact area (from a radius of 64 to 90 nm, respectively). For silica spheres interacting with cationically patchy surfaces at pH 6, simulations revealed that 20–100 patches were needed inside the zone of influence to capture flowing microspheres [29]. The smaller thresholds seen in Fig. 5A with bacteria suggest fewer patches need to trap flowing *S. aureus*, but still in a similar range.

4.4. Influence of flow

Fig. 8 explores the influence of flow on bacterial adhesion to albumin films containing different densities of cationic patches. Depending on the patch density, the flow produces different effects: increases in gentle shear tend to increase the rate of bacterial deposition, while higher shear rates inhibit bacterial capture. The crossover from shear-enhanced to shear-inhibited capture (i.e. the maximum capture rate as a function of shear) depends on the cationic patch density. These general features are borne out in Fig. 8A for bacterial adhesion on cationically patchy albumin films and in part B for silica sphere capture on the cationically-patchy silica flat. In interpreting these plots, it is important to note that the transport limited (maximum) bacterial deposition rate is

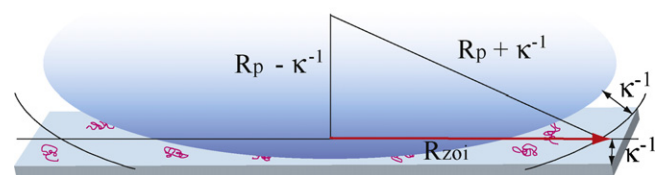


Fig. 7. Zone of influence: the amount of substrate within electrostatic reach of a rigid sphere. R_p is the sphere radius and κ^{-1} the Debye length. R_{zoi} is the radius of the zone of influence, from Ref. [25].

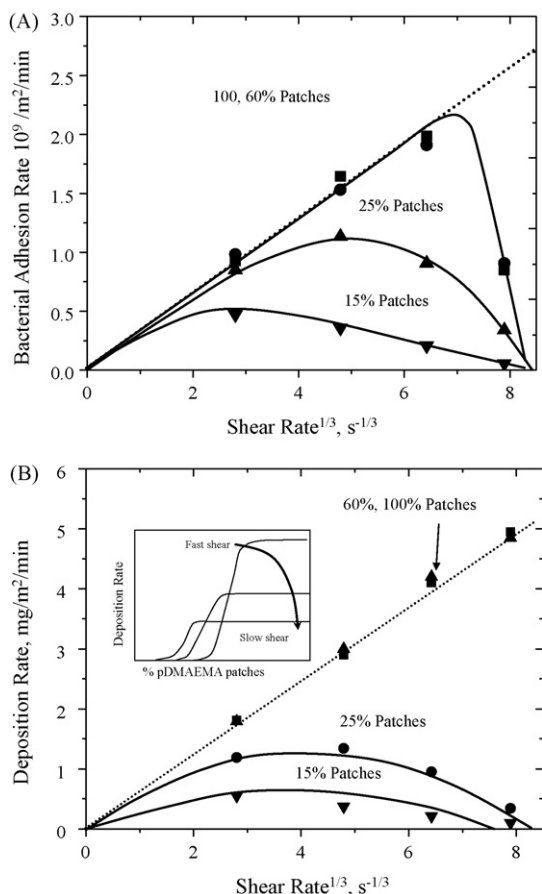


Fig. 8. (A) Deposition rates of *S. aureus* bacteria as a function of wall shear on BSA layers carrying different amounts of pDMAEMA patches at pH 7.4, 26 mM. (B) Deposition rates of 1 μm silica particles as a function of wall shear on silica flats carrying different amounts of pDMAEMA patches at pH 7.4, 26 mM. The inset shows the shifting of the thresholds and transport-limited plateau rates for the same system at pH 6.1, from Ref. [27]. At pH 6.1, the deposition rate as a function of shear rate was qualitatively similar to the behavior seen in the main part of the graph at pH 7.4, in the current study, suggesting a similar overall pattern for the current data.

indicated by the diagonal line. While the data for the 15% and 25% surfaces fall below this limit, it is clear that at the lowest shear rates they must ultimately follow the diagonal. This necessarily imparts a maximum to the 15% data set, below 22 s^{-1} .

This crossover in the influence of flow has been reported previously for systems in which the surface density of adhesive elements is varied [10,43]. For instance, Mohamed et al. [43] reported maxima in *S. aureus* deposition from flow with variations in flow rate, when several populations of bacteria were compared. Bacteria were grown under conditions that varied the density of collagen receptors from 2800 to 8000/cell, and the deposition from flow onto collagen films was studied. The most rapid deposition was observed for the strain with the greatest receptor density. At the opposite extreme with the strain with the lowest density of collagen receptors, deposition was slower and flow mostly detracted from bacterial capture. The shear corresponding to the maximum bacterial deposition increased with increasing receptor density, similar to Fig. 8. The parallel between that study and Fig. 8 is particularly interesting since in our study, the adhesive elements were on the substrate while in Mohamed's study, the variations of receptors were on the bacteria themselves. The comparison also demonstrates separately that our findings for heterogeneous surfaces translate to heterogeneous particles, both synthetic and biological.

The data in Fig. 8B for silica spheres interacting with a patchy surface at pH 7.4 closely resemble the behavior of the same system

at pH 6.1 which was studied in more detail. In that previous work, and included schematically in the inset of Fig. 8B, it was shown that flow shifts both the transport-limited plateau and the threshold itself. Therefore, at fixed composition, one crosses between surface-controlled and transport-limited shear dependencies. The surface-controlled bacterial deposition is indeed reduced as shear forces increase, as one might expect [44]. We expect a similar explanation to hold for bacterial adhesion.

A comparison of Fig. 8A and B, reveals remarkable quantitative similarity between bacterial and silica sphere capture over a broad range of surface compositions and flow rates, with the exception of the highest shear rates. At wall shear rates approaching 500 s^{-1} , bacterial adhesion is reduced on the most adhesive fully cationic surfaces. In Fig. 8B, transport-limited capture of silica spheres extends beyond 500 s^{-1} on the strongly adhesive surfaces. The contrast suggests fundamental differences in the bacterial adhesion and silica particle capture at the strongest shear forces. For a 1 μm sphere to be captured on a surface in water flowing at a wall shear of 500 s^{-1} , the sphere must resist shear forces of 4 pN [45,46]. The data in Fig. 8A show that on the most adhesive surfaces (with 60 and 100% cationic coverage, bacteria adhere at the transport limited rate from a wall shear of 275 s^{-1} , i.e. surface forces are able to resist the 2.2 pN shear. When the shear is increased to 500 s^{-1} , however, surface forces cannot hold the bacteria in the 4 pN shear field. This magnitude of force for bacterial capture is entirely consistent with previous reports of the forces involved with bacterial capture [10–12,44,47]. We see here, through the contrast with silica particles, however, that electrostatics alone should be able to overcome the shear, which is not the case for bacteria. This suggests some (1) restructuring of the bacterial surface in the failure to “hang onto” the surface, (2) a short range steric barrier preventing close approach, since the electrostatic interactions are otherwise quite similar, as evidenced by the zeta potential data in Fig. 6, or (3) a lack of strong van der Waals interactions with the underlying flat, due to the watery nature of the bacterial particle itself, compared with solid silica spheres.

5. Conclusions and significance

This work probed the adhesion of *S. aureus* to protein films with cationic heterogeneity on the lengthscale from 10 to 100 nm. Similar adhesion of bacteria or silica spheres on their respective model substrates included a threshold in the amount of polycation coils needed for adhesion, indicating the involvement of several polycation patches at once, “multivalent binding”. The adhesion threshold shifted to greater surface patch densities at reduced ionic strength, consistent with an adhesion mechanism dependent on the electrostatic contact area between the bacterium and the surface. At high ionic strength or for small contact areas, bacterial capture became highly sensitive to statistical clusters of the polycations, producing adhesion of negative bacteria on net negative surfaces. While other interactions such as hydrogen bonding, hydrophobicity, or van der Waals forces might be part of an explanation, the close similarity of bacterial deposition to the silica particle system suggests that the bacterial capture can be explained by charge heterogeneity, alone.

This study also documented a parallel between the wall shear effect on bacterial and silica particle deposition on electrostatically patchy surfaces. With small but sufficient patches for particle/bacteria capture, increased flow made capture more difficult. On the surfaces containing dense cationic functionality, bacterial and silica particle capture was enhanced by flow, via increased transport. The crossover between the flow-enhanced and flow-inhibited capture shifted to higher flow rates with increases in the cationic patch density.

One marked contrast between bacterial adhesion and silica particle capture occurred at the strongest shear rates, 500 s^{-1} . Here, on the densely functionalized cationically patchy surfaces, silica particle capture proceeded at the transport limited rate, demonstrating that surface forces were able to hold particles against shear forces near 4 pN . This was not the case for bacterial adhesion which was compromised at these conditions. The bacterial adhesion was able to resist shear up to 2.75 pN , but not much above this level. This indicates weaker bacterial binding to these cationic surfaces, possibly as a result of surface restructuring of the bacteria during short term contact with the surface, or an inability to make complete contact (i.e. access the deepest part of the minimum in the particle-surface potential), perhaps due to short-range steric repulsions.

Acknowledgements

This work was initiated with the support of NSF CBET-0428455 and completed under support from NSF DMR-0805061, and NSF CHE-0221791 (to K.N.).

References

- [1] N. Tufenkji, M. Elimelech, Breakdown of colloid filtration theory: role of the secondary energy minimum and surface charge heterogeneities, *Langmuir* 21 (2005) 841–852.
- [2] J.A. Redman, S.L. Walker, M. Elimelech, Bacterial adhesion and transport in porous media: role of the secondary energy minimum, *Environmental Science & Technology* 38 (2004) 1777–1785.
- [3] S.L. Walker, J.A. Redman, M. Elimelech, Role of cell surface lipopolysaccharides in *Escherichia coli* K12 adhesion and transport, *Langmuir* 20 (2004) 7736–7746.
- [4] S.L. Walker, J.E. Hill, J.A. Redman, M. Elimelech, Influence of growth phase on adhesion kinetics of *Escherichia coli* D21g, *Applied and Environmental Microbiology* 71 (2005) 3093–3099.
- [5] S. Kang, E.M.V. Hoek, H. Choi, H. Shin, Effect of membrane surface properties during the fast evaluation of cell attachment, *Separation Science and Technology* 41 (2006) 1475–1487.
- [6] E.M.V. Hoek, S. Bhattacharjee, M. Elimelech, Effect of membrane surface roughness on colloid-membrane DLVO interactions, *Langmuir* 19 (2003) 4836–4847.
- [7] S. Walker, M. Elimelech, J. Redman, Influence of growth phase on bacterial deposition: interaction mechanisms in packed-bed column and radial stagnation point flow systems (Vol 39, Pg 6405, 2005), *Environmental Science & Technology* 40 (2006) 5586–15586.
- [8] S. Wang, G. Guillen, E.M.V. Hoek, Direct observation of microbial adhesion to membranes, *Environmental Science & Technology* 39 (2005) 6461–6469.
- [9] S.T. Kang, A. Subramani, E.M.V. Hoek, M.A. Deshusses, M.R. Matsumoto, Direct observation of biofouling in cross-flow microfiltration: mechanisms of deposition and release, *Journal of Membrane Science* 244 (2004) 151–165.
- [10] N.P. Boks, W. Norde, H.C. van der Mei, H.J. Busscher, Forces involved in bacterial adhesion to hydrophilic and hydrophobic surfaces, *Microbiology-Sgm* 154 (2008) 3122–3133.
- [11] M.P. Tong, T.A. Camesano, W.P. Johnson, Spatial variation in deposition rate coefficients of an adhesion-deficient bacterial strain in quartz sand, *Environmental Science & Technology* 39 (2005) 3679–3687.
- [12] N.P. Boks, H.J. Busscher, H.C. van der Mei, W. Norde, Bond-strengthening in staphylococcal adhesion to hydrophilic and hydrophobic surfaces using atomic force microscopy, *Langmuir* 24 (2008) 12990–12994.
- [13] C.P. Xu, B. van de Belt-Gritter, R.J.B. Dijkstra, W. Norde, H.C. van der Mei, H.J. Busscher, Interaction forces between salivary proteins and *Streptococcus mutans* with and without antigen I/II, *Langmuir* 23 (2007) 9423–9428.
- [14] K. Vacheethasane, J.S. Temenoff, J.M. Higashi, A. Gary, J.M. Anderson, R. Bayston, R.E. Marchant, Bacterial surface properties of clinically isolated *Staphylococcus epidermidis* strains determine adhesion on polyethylene, *Journal of Biomedical Materials Research* 42 (1998) 425–432.
- [15] A. Atabek, T.A. Camesano, Atomic force microscopy study of the effect of lipopolysaccharides and extracellular polymers on adhesion of *Pseudomonas aeruginosa*, *Journal of Bacteriology* 189 (2007) 8503–8509.
- [16] R.J. Emerson, T.S. Bergstrom, Y.T. Liu, E.R. Soto, C.A. Brown, W.G. McGimpsey, T.A. Camesano, Microscale correlation between surface chemistry, texture, and the adhesive strength of *Staphylococcus epidermidis*, *Langmuir* 22 (2006) 11311–11321.
- [17] Y.T. Liu, J. Strauss, T.A. Camesano, Thermodynamic investigation of *Staphylococcus epidermidis* interactions with protein-coated substrata, *Langmuir* 23 (2007) 7134–7142.
- [18] N.I. Abu-Lail, T.A. Camesano, Specific and nonspecific interaction forces between *Escherichia coli* and silicon nitride, determined by Poisson statistical analysis, *Langmuir* 22 (2006) 7296–7301.
- [19] N.I. Abu-Lail, T.A. Camesano, Role of lipopolysaccharides in the adhesion, retention, and transport of *Escherichia coli* Jm109, *Environmental Science & Technology* 37 (2003) 2173–2183.
- [20] C.P. Xu, N.P. Boks, J. de Vries, H.J. Kaper, W. Norde, H.J. Busscher, H.C. van der Mei, *Staphylococcus aureus*-fibrinectin interactions with and without fibronectin-binding proteins and their role in adhesion and desorption, *Applied and Environmental Microbiology* 74 (2008) 7522–7528.
- [21] H.J. Busscher, B. van de Belt-Gritter, R.J.B. Dijkstra, W. Norde, F.C. Petersen, A.A. Scheie, H.C. van der Mei, Intermolecular forces and enthalpies in the adhesion of *Streptococcus mutans* and an antigen I/II-deficient mutant to laminin films, *Journal of Bacteriology* 189 (2007) 2988–2995.
- [22] H.J. Busscher, B. van de Belt-Gritter, R.J.B. Dijkstra, W. Norde, H.C. van der Mei, *Streptococcus mutans* and *Streptococcus intermedius* adhesion to fibrinectin films are oppositely influenced by ionic strength, *Langmuir* 24 (2008) 10968–10973.
- [23] P.J. Wit, H.J. Busscher, Site selectivity in the deposition and redeposition of polystyrene particles to glass, *Journal of Colloid and Interface Science* 208 (1998) 351–352.
- [24] N. Kozlova, M.M. Santore, Manipulation of micrometer-scale adhesion by tuning nanometer-scale surface features, *Langmuir* 22 (2006) 1135–1142.
- [25] M.M. Santore, N. Kozlova, Micrometer scale adhesion on nanometer-scale patchy surfaces: adhesion rates, adhesion thresholds, and curvature-based selectivity, *Langmuir* 23 (2007) 4782–4791.
- [26] Y.W. Shin, J.E. Roberts, M.M. Santore, The relationship between polymer/substrate charge density and charge overcompensation by adsorbed polyelectrolyte layers, *Journal of Colloid and Interface Science* 247 (2002) 220–230.
- [27] Y. Shin, J.E. Roberts, M.M. Santore, Influence of charge density and coverage on bound fraction for a weakly cationic polyelectrolyte adsorbing onto silica, *Macromolecules* 35 (2002) 4090–4095.
- [28] G.J. Fleer, M.A. Cohen Stuart, J.M.H.M. Schoutjens, T. Cosgrove, B. Vincent, *Polymers at Interfaces*, Chapman and Hall, London, 1993.
- [29] R. Duffadar, S. Kalasin, J.M. Davis, M.M. Santore, The impact of nanoscale chemical features on micron-scale adhesion: crossover from heterogeneity-dominated to mean-field behavior, *Journal of Colloid and Interface Science* 337 (2009) 396–407.
- [30] N. Hansupalak, M.M. Santore, Sharp polyelectrolyte adsorption cutoff induced by a monovalent salt, *Langmuir* 19 (2003) 7423–7426.
- [31] N. Hansupalak, M.M. Santore, Polyelectrolyte desorption and exchange dynamics near the sharp adsorption transition: weakly charged chains, *Macromolecules* 37 (2004) 1621–1629.
- [32] M.M. Santore, J. Zhang, S. Srivastava, V.M. Rotello, Beyond molecular recognition: using a repulsive field to tune interfacial valency and binding specificity between adhesive surfaces, *Langmuir* 25 (2009) 84–96.
- [33] S. Kalasin, M.M. Santore, Hydrodynamic crossover in dynamic microparticle adhesion on surfaces of controlled nanoscale heterogeneity, *Langmuir* 24 (2008) 4435–4438.
- [34] S. Kalasin, M.M. Santore, Non-specific adhesion on biomaterial surfaces driven by small amounts of protein adsorption, *Colloids and Surfaces B-Biointerfaces* 73 (2009) 229–236.
- [35] Z.G. Fu, M.M. Santore, Poly(ethylene oxide) adsorption onto chemically etched silicates by Brewster angle reflectivity, *Colloids and Surfaces A-Physicochemical and Engineering Aspects* 135 (1998) 63–75.
- [36] A. Toscano, M.M. Santore, Fibrinogen adsorption on three silica-based surfaces: conformation and kinetics, *Langmuir* 22 (2006) 2588–2597.
- [37] C.T. Shibata, A.M. Lenhoff, T. Tirf, Effect of salt and surface effects on protein adsorption. 1. Equilibrium, *Journal of Colloid and Interface Science* 148 (1992) 469–484.
- [38] N.P. Boks, H.J. Kaper, W. Norde, H.C. van der Mei, H.J. Busscher, Mobile and immobile adhesion of staphylococcal strains to hydrophilic and hydrophobic surfaces, *Journal of Colloid and Interface Science* 331 (2009) 60–64.
- [39] A. Roosjen, N.P. Boks, H.C. van der Mei, H.J. Busscher, W. Norde, Influence of shear on microbial adhesion to peo-brushes and glass by convective-diffusion and sedimentation in a parallel plate flow chamber, *Colloids and Surfaces B-Biointerfaces* 46 (2005) 1–6.
- [40] C.F. Wertz, M.M. Santore, Adsorption and relaxation kinetics of albumin and fibrinogen on hydrophobic surfaces: single-species and competitive behavior, *Langmuir* 15 (1999) 8884–8894.
- [41] C.F. Wertz, M.M. Santore, Effect of surface hydrophobicity on adsorption and relaxation kinetics of albumin and fibrinogen: single-species and competitive behavior, *Langmuir* 17 (2001) 3006–3016.
- [42] M.A. Leveque, *Annales des Mines* 13 (1928) 284.
- [43] N. Mohamed, T.R. Rainier, J.M. Ross, Novel experimental study of receptor-mediated bacterial adhesion under the influence of fluid shear, *Biotechnology and Bioengineering* 68 (2000) 628–636.
- [44] R.B. Dickinson, J.A. Nagel, D. McDevitt, T.J. Foster, R.A. Proctor, S.L. Couper, Quantitative comparison of clumping factor-mediated and coagulase-mediated *Staphylococcus aureus* adhesion to surface-bound fibrinogen under flow, *Infection and Immunity* 63 (1995) 3143–3150.
- [45] A.J. Goldman, R.G. Cox, H. Brenner, Slow viscous motion of a sphere parallel to a plane wall. I. Motion through a quiescent fluid, *Chemical Engineering Science* 22 (1967) 637.
- [46] A.J. Goldman, R.G. Cox, H. Brenner, Slow viscous motion of a sphere parallel to a plane wall. 2. Couette flow, *Chemical Engineering Science* 22 (1967) 653.
- [47] H.J. Busscher, H.C. van der Mei, Microbial adhesion in flow displacement systems, *Clinical Microbiology Reviews* 19 (2006) 127.